BMCs recruited into the infarcted myocardium may contain various kinds of somatic stem cells, such as endothelial progenitor cells [20], bone marrow-derived stem cells [21], and bone marrow mononuclear cells [2], which have potent therapeutic effects in heart failure [22]. Furthermore, bone marrow-derived mesenchymal stem cells secrete prostaglandin [23], which may act like ONO-1301 and amplify the effects of the ONO-1301-mediated therapy. Kawabe et al. clearly showed that prostaglandin facilitates the recruitment of endothelial progenitor cells [24]. Although further analysis is needed, the enhanced accumulation of BMCs may predispose the damaged heart tissue to better restoration following MI.

Many reports have shown that granulocyte colony-stimulating factor (G-CSF) and granulocyte-macrophage colony-stimulating factor (GM-CSF) also induce BMC mobilization, with therapeutic effects in animal models [25]. However, G-CSF therapy in unselected patients with acute MI did not lead to functional improvements beyond those achieved with conventional therapy. In addition, the administration of GM-CSF in cancer patients has been shown to transiently increase the LV end-systolic dimensions and decrease cardiac contractility [25,26]. The lack of efficacy of G-CSF therapy in clinical trials may be due, at least in part, to its poor initiation and duration; such therapies are likely to be most beneficial during the early phase after acute MI. Although conventional prostacyclin and its analogs are chemically and biologically unstable, ONO-1301 is a long-acting prostacyclin agonist that exerts stable effects *in vivo*, because it lacks a prostanoid structure. Furthermore, we used a slow-release form of ONO-1301, made by polymerizing it with poly-lactic and glycolic acid; this ONO-1301 could still be detected in the blood 3 weeks after its administration (figure S4 in File S1).

Furthermore, in our *in vitro* analysis, although we used normal human dermal fibroblasts to examine the SDF-1/CXCR-4-dependent BMC migration, the reactivity to ONO-1301 stimulation will differ depending on the cell type. For example, the G-CSF expression was upregulated in some kinds of cells (unpublished data). Thus, together with the upregulation of multiple beneficial cytokines such as HGF and VEGF, because of the longer duration of its activity, ONO-1301 may be more potent than conventional protein-based therapies.

Our data showed that ONO-1301 treatment was a potent inducer of BMC homing. Of the BMCs that accumulated in the infarcted myocardium, 43 percent expressed isolectin, an endothelial cell marker, but the other BMCs had a fibroblastic morphology, and did not express cardiac-lineage or cardiofibroblast markers (Figure S3 in File S1). ONO-1301 administration resulted in the attenuation of cardiac dysfunction, with enhanced BMC accumulation. Further study is required to elucidate the mechanism, but we speculate that paracrine effects of factors released by the BMCs play pivotal roles in the therapeutic efficacy, rather than the transdifferentiation of the BMCs into the cardiac or vascular lineage. The effect of cardioprotective and angiogenic factors secreted by the accumulated BMCs and the direct stimulation of ONO-1301 itself may synergistically increase the angiogenesis and cardioprotection, leading to improved therapeutic results.

In summary, ONO-1301 may be a powerful, long-acting activator of multiple cytokines. In particular, SDF-1 may enhance the BMC accumulation in a SDF-1/CXCR4-signaling-dependent manner, leading to an attenuation of the cardiac dysfunction following MI. Our findings suggest that the method involving a sustained release of ONO-1301 may be adapted as a novel drug delivery system for treating heart failure.

Supporting Information

File S1.
(DOCX)

Acknowledgments

We thank Masako Yokoyama and Akima Harada for their excellent technical assistance.

Author Contributions

Conceived and designed the experiments: YI SM Y. Sawa. Performed the experiments: YI KI NS. Analyzed the data: YI AS. Contributed reagents/materials/analysis tools: Y. Sakai. Wrote the paper: YI SM SF Y. Sawa.

References

1. Abbott JD (2004) Stromal cell-derived factor-1 plays a critical role in stem cell recruitment to the heart after myocardial infarction but is not sufficient to induce homing in the absence of injury. Circulation 110: 3300–3305.
2. Askari AT, Unzek S, Popovic ZB, Goldman CK, Forudi F, et al. (2003) Effect of stromal-cell-derived factor 1 on stem-cell homing and tissue regeneration in ischaemic cardiomyopathy. Lancet 362: 697–703.
3. Peled A (1999) Dependence of human stem cell engraftment and repopulation of NOD/SCID mice on CXCR4. Science 283: 845–848.
4. Yamaguchi Ji (2003) Stromal cell-derived factor-1 effects on ex vivo expanded endothelial progenitor cell recruitment for ischemic neovascularization. Circulation 107: 1322–1328.
5. Yamanaka S, Miura K, Yukimura T, Okumura M, Yamamoto K (1992) Putative mechanism of hypotensive action of platelet-activating factor in dogs. Circ Res 70: 893–901.
6. Sata M, Nakamura K, Iwata H, Sakai Y, Hirata Y, et al. (2007) A synthetic small molecule, ONO-1301, enhances endogenous growth factor expression and augments angiogenesis in the ischaemic heart. Clin Sci 112: 607.
7. Hirata Y, Soeki T, Akaike M, Sakai Y, Igarashi T, et al. (2009) Synthetic prostacycline agonist, ONO-1301, ameliorates left ventricular dysfunction and cardiac fibrosis in cardiomyopathic hamsters. Biomed Pharmacother 63: 781–786.
8. Yamasaki H, Maeshima Y, Nasu T, Saito D, Tanabe K, et al. (2011) Intermittent administration of a sustained-release prostacyclin analog ONO-1301 ameliorates renal alterations in a rat type 1 diabetes model. Prostaglandins Leukot Essent Fatty Acids 84: 99–107.
9. Nakamura K, Sata M, Iwata H, Sakai Y, Hirata Y, et al. (2007) A synthetic small molecule, ONO-1301, enhances endogenous growth factor expression and augments angiogenesis in the ischaemic heart. Clin Sci 112: 607–616.
10. Imanishi Y, Saito A, Komoda H, Kitagawa-Sakakida S, Miyagawa S, et al. (2008) Allogenic mesenchymal stem cell transplantation has a therapeutic effect in acute myocardial infarction in rats. J Mol Cell Cardiol 44: 662–671.
11. Imanishi Y, Miyagawa S, Maeda N, Fukushima S, Kitagawa-Sakakida S, et al. (2011) Induced adipocyte cell-sheet ameliorates cardiac dysfunction in a mouse myocardial infarction model: a novel drug delivery system for heart failure. Circulation 124: S10–17.
12. Ceradini DJ, Kulkarni AR, Callaghan MJ, Tepper OM, Bastidas N, et al. (2004) Progenitor cell trafficking is regulated by hypoxic gradients through HIF-1 induction of SDF-1. Nat Med 10: 858–864.
13. Zaruba MM, Franz WM (2010) Role of the SDF-1-CXCR4 axis in stem cell-based therapies for ischemic cardiomyopathy. Expert Opin Biol Ther 10: 321–335.
14. Goichberg P (2005) cAMP-induced PKCzeta activation increases functional CXCR4 expression on human CD34+ hematopoietic progenitors. Blood 107: 870–879.
15. North TE, Goessling W, Walkley CR, Lengerke C, Kopani KR, et al. (2007) Prostaglandin E2 regulates vertebrate haematopoietic stem cell homeostasis. Nature 447: 1007–1011.
16. Leri A, Kajstura J, Anversa P (2011) Role of cardiac stem cells in cardiac pathophysiology: a paradigm shift in human myocardial biology. Circ Res 109: 941–961.
17. Smith RR, Barile L, Cho HC, Leppo MK, Hare JM, et al. (2007) Regenerative potential of cardiosphere-derived cells expanded from percutaneous endomyocardial biopsy specimens. Circulation 115: 896–908.
18. Mollova M, Bersell K, Walsh S, Savla J, Das LT, et al. (2013) Cardiomyocyte proliferation contributes to heart growth in young humans. Proc Nat Acad Sci U S A 110: 1446–1451.

19. Kajstura J, Rota M, Cappetta D, Ogorek B, Arranto C, et al. (2012) Cardiomyogenesis in the aging and failing human heart. Circulation 126: 1869–1881.
20. Asahara T, Murohara T, Sullivan A, Silver M, van der Zee R, et al. (1997) Isolation of putative progenitor endothelial cells for angiogenesis. Science 275: 964–967.
21. Orlic D, Kajstura J, Chimenti S, Limana F, Jakoniuk I, et al. (2001) Mobilized bone marrow cells repair the infarcted heart, improving function and survival. Proc Natl Acad Sci U S A 98: 10344–10349.
22. Smart N, Riley PR (2008) The stem cell movement. Circ Res 102: 1155–1168.
23. Matysiak M, Orlowski W, Fortak-Michalska M, Jurewicz A, Selmaj K (2011) Immunoregulatory function of bone marrow mesenchymal stem cells in EAE depends on their differentiation state and secretion of PGE2. J Neuroimmunol 233: 106–111.
24. Kawabe J, Yuhki K, Okada M, Kanno T, Yamauchi A, et al. (2010) Prostaglandin I2 promotes recruitment of endothelial progenitor cells and limits vascular remodeling. Arterioscler Thromb Vasc Biol 30: 464–470.
25. Sanganalmath SK, Abdel-Latif A, Bolli R, Xuan YT, Dawn B (2011) Hematopoietic cytokines for cardiac repair: mobilization of bone marrow cells and beyond. Basic Res Cardiol 106: 709–733.
26. Knoops S, Groeneveld ABJ, Kamp O, Lagrand WK, Hoekman K (2001) Granulocyte-macrophage colony-stimulating factor (GM-CSF) decreases left ventricular function. an echocardiographic study in cancer patients. Cytokine 14: 184–187.

Cardiovascular Research (2013) **99**, 102–110
doi:10.1093/cvr/cvt088

Transplantation of myoblast sheets that secrete the novel peptide SVVYGLR improves cardiac function in failing hearts

Ayako Uchinaka[1], Naomasa Kawaguchi[1,2*], Yoshinosuke Hamada[1], Seiji Mori[1], Shigeru Miyagawa[3], Atsuhiro Saito[4], Yoshiki Sawa[3], and Nariaki Matsuura[1]

[1]Department of Molecular Pathology, Osaka University Graduate School of Medicine, Suita, Japan; [2]Department of Cardiovascular Pathology, Division of Health Sciences, Osaka University Graduate School of Medicine, Suita, Japan; [3]Department of Cardiovascular Surgery, Osaka University Graduate School of Medicine, Suita, Japan; and [4]Medical Center of Translational Research, Osaka University Hospital, Osaka University Graduate School of Medicine, Suita, Japan

Received 4 December 2012; revised 27 March 2013; accepted 7 April 2013; online publish-ahead-of-print 23 April 2013

Time for primary review: 52 days

Aims Transplantation of myoblast sheets is a promising therapy for enhancing cardiac function after heart failure. We have previously demonstrated that a 7-amino-acid sequence (Ser-Val-Val-Tyr-Gly-Leu-Arg) derived from osteopontin (SV peptide) induces angiogenesis. In this study, we evaluated the long-term therapeutic effects of myoblast sheets secreting SV in a rat infarction model.

Methods and results Two weeks after ligation of the left anterior descending coronary artery, the animals were divided into the following three groups: a group transplanted with wild-type rat skeletal myoblast sheets (WT-rSkMs); a group transplanted with SV-secreting myoblast sheets (SV-rSkMs); and a control group (ligation only). We evaluated cardiac function, histological changes, and smooth muscle actin (SMA) expression through transforming growth factor-β (TGF-β) signalling. The ejection fraction and fractional shortening were significantly better, and the enlargement of end-systolic volume was also significantly attenuated in the SV-rSkM group. Left ventricular remodelling, including fibrosis and hypertrophy, was significantly attenuated in the SV-rSkM group, and SV secreted by the myoblast sheets promoted angiogenesis in the infarcted border area. Furthermore, many clusters of SMA-positive cells were observed in the infarcted areas in the SV-rSkM group. *In vitro* SMA expression was increased when SV was added to the isolated myocardial fibroblasts. Moreover, SV bound to the TGF-β receptor, and SV treatment activated TGF-β receptor–Smad signalling.

Conclusion The SV-secreting myoblast sheets facilitate a long-term improvement in cardiac function. The SV can induce differentiation of fibroblasts to myofibroblasts via TGF-β–Smad signalling. This peptide could possibly be used as a bridge to heart transplantation or as an ideal peptide drug for cardiac regeneration therapy.

Keywords Cell therapy • Peptides • Myocardial infarction • Myofibroblats • Transforming growth factor-β

1. Introduction

In heart failure, tissue damage processes caused by ischaemia, such as cell death, fibrosis, and hypertrophy, gradually progress until the cardiac tissue becomes dysfunctional.[1–3] Transplantation of myoblast sheets is a promising treatment for ischaemic heart failure, and can inhibit left ventricular (LV) remodelling and improve cardiac function via paracrine effectors.[4–8] The cell-sheet technique avoids the arrhythmogenicity associated with skeletal myoblast therapy by injection.[9]

However, this treatment has failed to achieve long-term therapeutic effects, because the transplanted sheets are exposed to blood and nutrient deprivation and drop out from the injured myocardium. Recent studies demonstrated that myoblast sheets that overexpress different cardioprotective agents display enhanced therapeutic effects.[10,11] Therefore, the combined application of gene therapy with angiogenic agents and myoblast sheet transplantation may achieve sustained therapeutic efficacy. Through the secretion of angiogenic factors from transplanted myoblasts, the newly formed blood vessels can supply blood flow to the surviving myocardium and the transplanted

* Corresponding author: 1-7 Yamada-oka, Suita, Osaka 565-0871, Japan. Tel: +81 6 6879 2588; fax: +81 6 6879 2588, E-mail: kawaguch@sahs.med.osaka-u.ac.jp
Published on behalf of the European Society of Cardiology. All rights reserved. © The Author 2013. For permissions please email: journals.permissions@oup.com.

Downloaded from http://cardiovascres.oxfordjournals.org/ at Osaka University on March 11, 2014

cells, and the functional deterioration of ischaemic cardiomyopathy should thus improve in the long term.

Osteopontin is a multifunctional cytokine expressed during healing and fibrotic processes.[12] We have previously reported that the osteopontin-derived peptide Ser-Val-Val-Tyr-Gly-Leu-Arg (SVVYGLR; SV) exhibits angiogenic activity *in vitro* and *in vivo*,[13–17] and that its angiogenic activity is as potent as that of vascular endothelial growth factor (VEGF).[14] Owing to their high molecular weights, the most well-known angiogenesis-promoting factors, namely, VEGF and hepatocyte growth factor (HGF), are resistant to degradation. In contrast, peptides such as SV are more easily degraded by peptidase within an organism and show only a few adverse effects, such as oedema and pleural fluid accumulation.[18–20] This indicates the high biocompatibility of peptides.

In this study, we hypothesized that the augmentation of myoblast sheets by SV gene transfer could improve cardiac function in the long term.

2. Methods

2.1 Animal ethics

Animal care complied with the 'Guide for Care and Use of Laboratory Animals' (NIH publication no. 85-23, revised 1996). The Ethics Review Committee for Animal Experimentation of Osaka University Graduate School of Medicine approved the experimental protocols.

2.2 Isolation of skeletal myoblasts and sheets

After induction of general anaesthesia with pentobarbital (300 mg/kg) and heparin (150 U) by intraperitoneal injection, myoblasts were isolated from the skeletal muscle of the tibialis anterior muscle of 3-week-old male Lewis rats. The muscles were minced and enzymatically dissociated with 0.2% collagenase type II (Worthington Biochemical Corp., Lakewood, NJ, USA) and trypsin at 37°C. The isolated cells were suspended in Dulbecco's modified Eagle's medium with 20% fetal bovine serum. After being preplated twice, non-adherent cells were then plated on a dish coated with Matrigel (Becton Dickinson Bioscience, Franklin Lakes, NJ, USA) and incubated at 37°C in humidified air enriched with 5% CO_2. We maintained the cell densities at <70% confluence to prevent skeletal myoblast differentiation that would result in myotube formation. Myoblast sheets were formed by plating 3×10^6 infected myoblasts on a temperature-responsive culture dish (UpCell; CellSeed, Tokyo, Japan).

2.3 Animal model and myoblast sheet transplantation

The myocardial infarction (MI) models were generated via ligation of the left anterior descending (LAD) coronary artery in 8-week-old female F344/NJcl-rnu/rnu rats. The rats were anaesthetized by inhalation of isoflurane (2%, 0.2 mL/min), intubated, and placed on a respirator during surgery to maintain ventilation. The carrier gas for isoflurane is oxygen. The adequacy of anaesthesia was monitored by electrocardiography and pulse rate. Two weeks after ligation of the LAD coronary artery, the myoblast sheets were transplanted. The rats were randomly divided into the following three groups: (i) a WT-rat skeletal myoblast (rSkM) group (transplanted with three wild-type myoblast sheets, $n = 6$); (ii) an SV-rSkM group (transplanted with three SV-secreting myoblast sheets, $n = 8$); and (iii) a control group (sham operation, $n = 6$). Each sheet was individually applied to the infarcted area.

2.4 Overexpression and transfection of SV

A lentiviral vector containing the complementary DNA (cDNA) of SV (SV/pCS-CG) was constructed (*Figure 1A*). The cDNA of SV was synthesized using DNA oligonucleotides. The primer sequences were as follows: forward, 1,5′-GCGCCACCATGGAGACAGACACACTCCTGCTATGG GTACTGCTGCTCTGGGTTCCAGGT-3′; forward, 2,5′-TCCACTGGT GACGCGGCCCAGCCGGCCAGTGTGGTTTATGGACTGAGGCTC GAGTACCCATACGATGTTCCAGATTACGCTTAAC-3′; reverse, 1,5′-TCGAGTTAAGCGTAATCTGGAACATCGTATGGGTACTCGA GCCTCAGTCCATAAACCACACT-3′; and reverse, 2,5′-GGCCGGC TGGGCCGCGTCACCAGTGGAACCTGGAACCCAGAGCAGCAGTA CCCATAGCAGGAGTGTGTCTGTCTCCATGGTGGCG-3′.

The synthesized DNA oligonucleotides were linked and ligated to pCS-CG, and the isolated rSkMs were infected via incubation for 48 h in the presence of SV/pCS-CG.

2.5 Dot blotting assay

The culture media were used for the assays. Each sample was coated onto a black 96-well microplate overnight. To evaluate the secretion SV volume, the serially diluted solution of SV-HA peptide was also coated onto the plate as a control. After blocking, the primary antibody against the HA tag (Santa Cruz Biotechnology, Santa Cruz, CA, USA) was added to each well. After washing, anti-rabbit IgG-linked horseradish peroxidase (GE Healthcare, Piscataway, NJ, USA) was added. After washing, the plate was exposed to an Enhanced Chemiluminescence (ECL) kit (GE Healthcare).

2.6 Measurement of cardiac function

The cardiac function of the treated rats was evaluated by echocardiography 2, 4, 6, and 8 weeks after sheet transplantation. Baseline measurements were

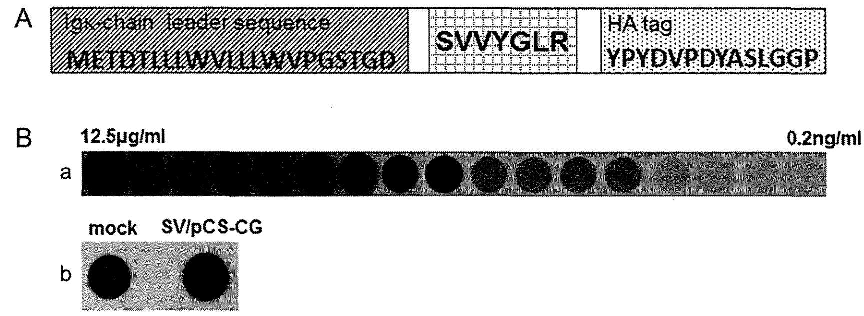

Figure 1 Assessment of SV expression. (*A*) View showing the frame format of the constructed SV gene. (*B*) Expression of SV in rSkMs infected with SV/pCS-CG by dot blotting: (*a*) the dilution series of SV-HA peptide; and (*b*) control cells infected with the empty vector (mock, left) and rSkMs infected with SV/pCS-CG (right).

Downloaded from http://cardiovascres.oxfordjournals.org/ at Osaka University on March 11, 2014

made before sheet transplantation. The measurements were made using a SONOS 5500 sonograph (Philips Electronics, Tokyo, Japan) with a 12 MHz transducer under general anaesthesia induced and maintained by inhalation of isoflurane (2%, 0.2 mL/min) as mentioned above. The LV end-systolic area, LV end-diastolic area, and LV dimensions at end diastole and end systole (LVIDd and LVIDs, respectively) were determined. The ejection fraction (EF), fractional shortening (FS), end-diastolic volume (EDV), and end-systolic volume (ESV) were calculated as follows:

$$\mathrm{LVEF}\ (\%) = (\mathrm{LVDd}^3 - \mathrm{LVDs}^3)/\mathrm{LVDd}^3 \times 100\ (\%)$$
$$\mathrm{LV\%FS} = [(\mathrm{LVDd} - \mathrm{LVDs})/\mathrm{LVDd}] \times 100\ (\%)$$
$$\mathrm{EDV} = \mathrm{LVIDd}^3 \times (0.98 \times \mathrm{LVIDd} + 5.90)\ (\mathrm{mL})$$
$$\mathrm{ESV} = \mathrm{LVIDs}^3 \times (1.14 \times \mathrm{LVIDs} + 4.18)\ (\mathrm{mL})$$

2.7 Heart weight/body weight ratio

The body weights (BW; in grams) of the rats were measured 8 weeks after sheet transplantation, after which the rats were anaesthetized with pentobarbital (300 mg/kg) and heparin (150 U) by intraperitoneal injection, and their hearts were rapidly removed and weighed (in milligrams). The heart weight (HW)/BW ratio was then calculated.

2.8 Histological analyses

Myocardial specimens were obtained 8 weeks post-transplantation. The formalin-fixed samples were embedded in paraffin. The LV chamber diameter and the anterior wall thickness were measured from sections stained with haematoxylin and eosin. Infarcted wall thickness, posterior wall thickness, and LV chamber diameter were measured with the scale loupe. The sections were evaluated morphologically using the NIS Elements system (Nikon, Tokyo, Japan). Sirius Red staining was used to detect fibrosis. The percentage of fibrosis was calculated from the fibrotic ratio in the infarct border area. Periodic acid–Schiff staining for cardiomyocyte hypertrophy was also performed. We randomly selected 100 cardiomyocytes and measured the two-point shortest axes at the level of the nucleus.

Immunohistochemical staining for von Willebrand factor antigen was used to label vascular endothelial cells to permit the counting of blood vessels. The sections were incubated with primary antibody against von Willebrand factor (rabbit polyclonal; Dako, Glostrup, Denmark). The sections were incubated with a biotinylated anti-rabbit IgG antibody (Dako) and further incubated with peroxidase-conjugated streptavidin (SA; GE Healthcare). Visualization was performed with biphenyl-3,3′,4,4′-tetramine solution (Sigma, St Louis, MO, USA). The stained vascular endothelial cells were counted under a light microscope.

The distribution of myofibroblast-like cells was evaluated by immunohistochemical staining with anti-smooth muscle actin (SMA) antibody (Dako) and anti-smooth muscle myosin heavy chain (SM-MHC) type 2 antibody (Abcam Ltd, Cambridge, UK). The SMA-positive cell density was calculated as SMA positive area/infarcted area × 100 (%).

2.9 Primary culture of adult ventricular fibroblasts

Cardiac fibroblasts (CFs) were isolated from 8-week-old adult male Sprague–Dawley rats 4 weeks after the induction of MI by LAD ligation. The hearts were excised from anaesthetized rats and quickly transferred to Hank's buffered salt solution. The minced left ventricular tissues were digested using 100 U/mL type II collagenase and 0.1% trypsin at 37°C. The cells were centrifuged and suspended in Dulbecco's modified Eagle's medium supplemented with 10% fetal bovine serum, and incubated at 37°C in humidified air enriched with 5% CO_2.

2.10 Immunofluorescence staining

The isolated fibroblasts were incubated with SV (10 μg/mL), SV random peptide (GYRVLSV; 10 μg/mL), or transforming growth factor-β1 (TGF-β1; 25 ng/mL) for 72 h. The cells were fixed with 4% paraformaldehyde and incubated with anti-SMA antibody followed by incubation with cyanine-3-conjugated anti-rabbit secondary antibody (GE Healthcare). The nuclei were stained with 4′,6-diamino-2-phenylindole (DAPI; Invitrogen Life Technologies, Grand Island, NY, USA), and the fluorescent signals were detected by fluorescence microscopy (ECLIPSE E600, Nikon).

2.11 Western blotting assay

The isolated fibroblasts were incubated with SV (10 μg/mL), SV random peptide (10 μg/mL), or TGF-β1 (25 ng/mL) for 72 h. The cells were suspended in lysis buffer (50 mM Tris at pH 8.0, 120 mM NaCl, 1 mM EDTA, and 0.5% Nonidet P-40). Proteins in whole-cell lysates were separated by SDS–PAGE, transferred to a polyvinylidene fluoride transfer membrane (Millipore, Billerica, MA, USA), and probed sequentially with antibodies against SMA and α-tubulin (Sigma). The blots were developed using an ECL kit.

To examine the activity of TGF-β receptor–Smad signalling induced by SV, the phosphorylation of Smad2, Smad3, and TGF-β receptor I (TβRI) was studied by western blotting. The isolated fibroblasts were incubated with SV (10 μg/mL), SV random peptide (10 μg/mL), or TGF-β1 (25 ng/mL) for 1 h. Primary antibodies against phospho-Smad2, phospho-Smad3, Smad2/3 (Cell Signaling Technology, Inc., Danvers, MA, USA), TβRI (phospho S165; Abcam), and α-tubulin were used.

2.12 Construction of recombinant transforming growth factor-β receptorII

A pcDNA3.1 vector containing the cDNA encoding TβRII (pcDNA3.1-TβRII) was constructed. The recombinant TβRII was produced by transfecting HEK 293T cells with pcDNA3.1-TβRII. The culture media containing recombinant TβRII were harvested. The purification of recombinant TβRII was done using immunoprecipitation with anti-TβRII antibody.

2.13 Biacore analysis

The binding of SV to TβRII was assessed by Biacore analysis. Biotinylated SVs were captured on SA-coated BIAcore SA sensor chips (GE Healthcare, Piscataway, NJ, USA). Ligands were diluted to 10 μg/mL and injected at 10 μL/mL. To correct for refractive index change, non-specific binding, and instrument drift, a reference flow cell contained the SA-coated surface only. The recombinant TβRII was diluted to 10 μg/mL in Hank's buffered salt solution and injected during the association phase for 5 min (30 μL/min).

2.14 *In situ* proximity ligation assay

The Duolink *in situ* proximity ligation assay (PLA; Olink Biosciences, Uppsala, Sweden) was performed according to the manufacturer's protocol. The isolated fibroblasts were incubated in the presence of SV-HA peptide or SV-HA random peptide (GYRVLSV; 1 μg/mL) for 1 h. The fixed fibroblasts were incubated with the following primary antibodies: rabbit polyclonal anti-TβRII (Abcam) and mouse monoclonal anti-HA (Nacalai Tesque). The cells were then incubated with PLA probes consisting of two secondary anti-rabbit and anti-mouse antibodies, each tagged with an oligonucleotide. A hybridization solution consisting of two oligonucleotide linkers complementary to each PLA probe was added to the cells. The isolated cells were incubated with a Duolink Ligation stock containing ligase and Duolink polymerase. In addition, the cells were incubated with a detection solution consisting of fluorescently labelled oligonucleotides that hybridize to the rolling circle amplification product. The PLA signal was visualized using fluorescence microscopy.

2.15 Statistical analyses

Data are presented as the means ± SEM. Cardiac function was analysed by repeated-measures analysis of variance (ANOVA) for differences across the entire time course, as well as one-way ANOVA, whereas the Tukey–Kramer *post hoc* test was used to examine significant differences at each time point. To assess the significance of the differences between individual groups for

Downloaded from http://cardiovascres.oxfordjournals.org/ at Osaka University on March 11, 2014

other data, statistical comparisons were performed using Student's unpaired *t*-test. $P < 0.05$ was considered statistically significant.

3. Results

3.1 Overexpression of SV in rat skeletal myoblasts

The signal strength of dots in wells coated with the culture medium of SV/pCS-CG-infected rSkMs was stronger than that of dots in wells coated with the culture medium of mock-infected rSkMs (*Figure 1B*[*b*]). The SV was synthesized and secreted by SV/pCS-CG-infected rSkMs. In addition, from the dilution series of SV-HA peptide, the secretion volume of SV was calculated to be approximately 3.125–6.25 ng/mL (*Figure 1B*[*a*]).

3.2 Effect of SV-secreting myoblast sheet on left ventricular function

Echocardiography revealed significantly better values of LVEF and %FS in the WT-rSkM and SV-rSkM groups compared with the control group at all time points after transplantation ($P < 0.01$). Although there were still significant differences between the control and WT-rSkM groups after the 4 week time point, the LVEF and %FS in the WT-rSkM group decreased dramatically. Furthermore, LVEF and %FS were significantly better in the SV-rSkM group at 2, 6, and 8 weeks after transplantation compared with the WT-rSkM group (2 and 6 weeks, $P < 0.05$; 8 weeks, $P < 0.01$; *Figure 2A* and *B*).

The evaluation of LVIDs illustrated the inhibition of dilatation in the SV-rSkM group in comparison with the control and WT-rSkM groups. In particular, at 6 and 8 weeks after transplantation LVIDs was significantly attenuated in the SV-rSkM group compared with the control group (6 weeks $P < 0.05$; 8 weeks $P < 0.01$; *Table 1*). The enlargement of ESV was also significantly attenuated in the SV-rSkM group compared with the control group at 6 and 8 weeks after transplantation (6 weeks, $P < 0.05$; 8 weeks, $P < 0.01$; *Table 1*). The increase in EDV was significantly inhibited in the SV-rSkM group compared with the control group only at 8 weeks after transplantation ($P < 0.05$; *Table 1*).

3.3 Heart weight/body weight ratio

We used the HW/BW ratio as an indicator of cardiac hypertrophy. The HW/BW ratio was significantly greater in the SV-rSkM group at 8 weeks after transplantation compared with the control and WT-rSkM groups ($P < 0.01$; *Figure 2C*).

3.4 Effect of SV-secreting myoblast sheet on left ventricular remodelling

Haematoxylin and eosin staining demonstrated thinning of the infarcted wall in the control and WT-rSkM groups, whereas the thickness of the infarcted wall was maintained in the SV-rSkM group (*Figure 2D* and *Table 2*). Statistical analysis demonstrated that the LV chamber of the SV-rSkM group was significantly less dilated that those of the control and WT-rSkM groups ($P < 0.05$; *Table 2*) and that the infarcted wall in the SV-rSkM group was significantly thicker than that in the control

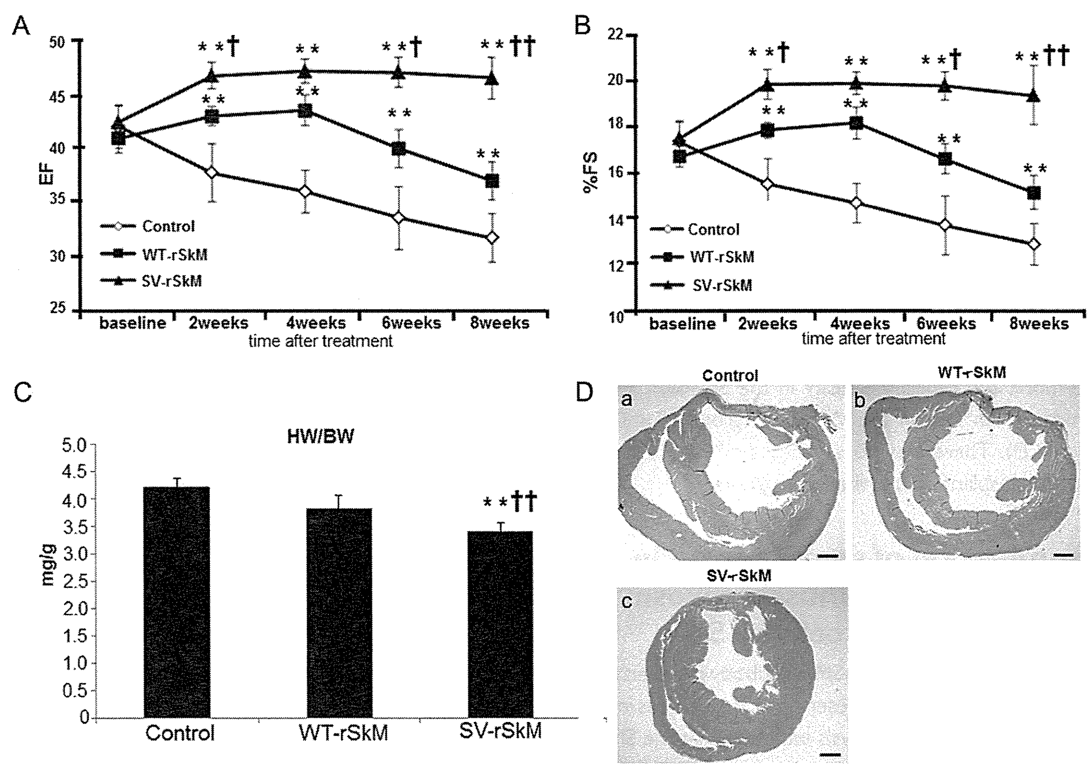

Figure 2 Echocardiographic evaluation of LV function after sheet transplantation (*A*, EF; *B*, %FS). $^{**}P < 0.01$ vs. Control group. $^{\dagger}P < 0.05$, $^{\dagger\dagger}P < 0.01$ vs. WT-rSkM group. Baseline is time of transplantation, which was 2 weeks after ligation of the LAD. Other times in weeks are post-transplantation. (*C*) Evaluation of HW/BW. $^{**}P < 0.01$ vs. Control group. $^{\dagger}P < 0.05$, $^{\dagger\dagger}P < 0.01$ vs. WT-rSkM group. (*D*) Haematoxylin- and eosin-stained section of the left ventricle: (*a*) control; (*b*) WT-rSkM; and (*c*) SV-rSkM (×10 magnification, scale bars represent 1000 μm).

Downloaded from http://cardiovascres.oxfordjournals.org/ at Osaka University on March 11, 2014

Table 1 Assessment of LVIDd, LVIDs, EDV, and ESV over time by echocardiography

	Baseline	2 weeks	4 weeks	6 weeks	8 weeks
LVIDd (cm)					
Control	0.75 ± 0.04	0.77 ± 0.07	0.81 ± 0.05	0.87 ± 0.04	0.89 ± 0.01
WT-rSkM	0.76 ± 0.02	0.77 ± 0.04	0.80 ± 0.06	0.84 ± 0.06	0.85 ± 0.03
SV-rSkM	0.71 ± 0.05	0.78 ± 0.07	0.78 ± 0.07	0.83 ± 0.03	0.84 ± 0.03*
LVIDs (cm)					
Control	0.63 ± 0.02	0.67 ± 0.05	0.70 ± 0.05	0.75 ± 0.04	0.77 ± 0.02
WT-rSkM	0.63 ± 0.02	0.64 ± 0.03	0.67 ± 0.06	0.69 ± 0.05	0.72 ± 0.04
SV-rSkM	0.64 ± 0.04	0.65 ± 0.05	0.67 ± 0.04	0.67 ± 0.03*	0.69 ± 0.04**
EDV (ml)					
Control	2.87 ± 0.46	3.19 ± 0.93	3.65 ± 0.71	4.46 ± 0.63	4.79 ± 0.26
WT-rSkM	2.93 ± 0.24	3.04 ± 0.43	3.53 ± 0.77	4.05 ± 0.89	4.22 ± 0.54
SV-rSkM	2.77 ± 0.53	3.26 ± 0.70	3.37 ± 0.64	3.92 ± 0.43	4.08 ± 0.43*
ESV (ml)					
Control	1.20 ± 0.13	1.49 ± 0.36	1.71 ± 0.34	2.16 ± 0.40	2.34 ± 0.23
WT-rSkM	1.25 ± 0.14	1.28 ± 0.16	1.53 ± 0.37	1.69 ± 0.33	1.88 ± 0.22
SV-rSkM	1.29 ± 0.21	1.39 ± 0.27	1.48 ± 0.25	1.51 ± 0.23*	1.61 ± 0.25**

Abbreviations: EDV, end-diastolic volume; ESV; end-systolic volume; LVIDd, left ventricular dimensions at end diastole; LVIDs, left ventricular dimensions at end systole. Baseline is the time of transplantation, which was 2 weeks after ligation of the left anterior descending coronary artery; other times in weeks are post-transplantation. *$P < 0.05$, **$P < 0.01$ vs. control group at each time point.

and WT-rSkM groups ($P < 0.01$; *Table 2*). The values of the LV chamber diameter/posterior wall thickness were significantly lower in the SV-rSkM group compared with those in the control and WT-rSkM groups ($P < 0.01$; *Table 2*). There were no significant differences between the control and WT-rSkM groups regarding these indices.

The SV-rSkM group exhibited a significantly lower percentage of fibrosis than the control and WT-rSkM groups in the infarcted border area ($P < 0.01$; *Figure 3A*). The diameters of cardiomyocytes in the SV-rSkM group were significantly smaller than those in the control and WT-rSkM groups ($P < 0.01$; *Figure 3B*). There was no significant difference in the area remote from the transplant among the three groups.

3.5 The pro-angiogenic effects of SV

The capillary density 8 weeks after transplantation was significantly higher in the WT-rSkM and SV-rSkM groups than in the control group ($P < 0.01$). Furthermore, the capillary density in the SV-rSkM group was significantly higher than that in the WT-rSkM group ($P < 0.01$; *Figure 3C[a]–C[c]* and *D*). There was no significant difference in the area remote from the transplant among the three groups.

3.6 The accumulation of smooth muscle actin-positive and smooth muscle myosin heavy chain type2-positive cells by SV

Immunohistochemical staining with an anti-SMA antibody revealed that many clusters of SMA-positive cells were present in infarcted areas in the SV-rSkM group (*Figure 3E*). Statistical analysis indicated that the SMA-positive cell density was significantly higher in the WT-rSkM and SV-rSkM groups than in the control group (WT-rSkM , $P < 0.05$; SV-rSkM, $P < 0.01$; *Figure 3F*). Furthermore, the SMA-positive cell density was significantly higher in the SV-rSkM group than in the WT-rSkM group ($P < 0.05$; *Figure 3F*). Notably, SM-MHC type 2-positive cells were also detected in infarcted areas in the SV-rSkM group, whereas those cells were scarce in the control and WT-rSkM groups (*Figure 3G*).

Table 2 Thickness of the infarcted wall and posterior wall and left ventricular chamber diameter

	Control	WT-rSkM	SV-rSkM
Left ventricular chamber diameter (mm)	4.50 ± 0.46	4.48 ± 0.42	3.85 ± 0.29**††
Infarcted wall thickness (mm)	0.53 ± 0.05	0.51 ± 0.08	0.63 ± 0.06
Posterior wall thickness (mm)	2.04 ± 0.10	1.88 ± 0.25	1.96 ± 0.14
Percentage anterior wall thickness	25.98 ± 2.66	27.20 ± 2.63	32.29 ± 0.98**††
Left ventricular chamber diameter/ posterior wall thickness	2.36 ± 0.22	2.30 ± 0.15	1.98 ± 0.16**††

The percentage anterior wall thickness is the infarcted wall thickness/posterior wall thickness × 100. **$P < 0.01$ vs. control group. ††$P < 0.01$ vs. WT-rSkM group.

3.7 The induction of smooth muscle actin by SV

Expression of SMA was increased when SV was added to the isolated fibroblasts (*Figure 4A* and *B*). The expression level of SMA was similar to that of TGF-β1 (*Figure 4B*). Conversely, the expression level of SMA was unchanged by the addition of SV random peptide (*Figure 4A* and *B*).

Downloaded from http://cardiovascres.oxfordjournals.org/ at Osaka University on March 11, 2014

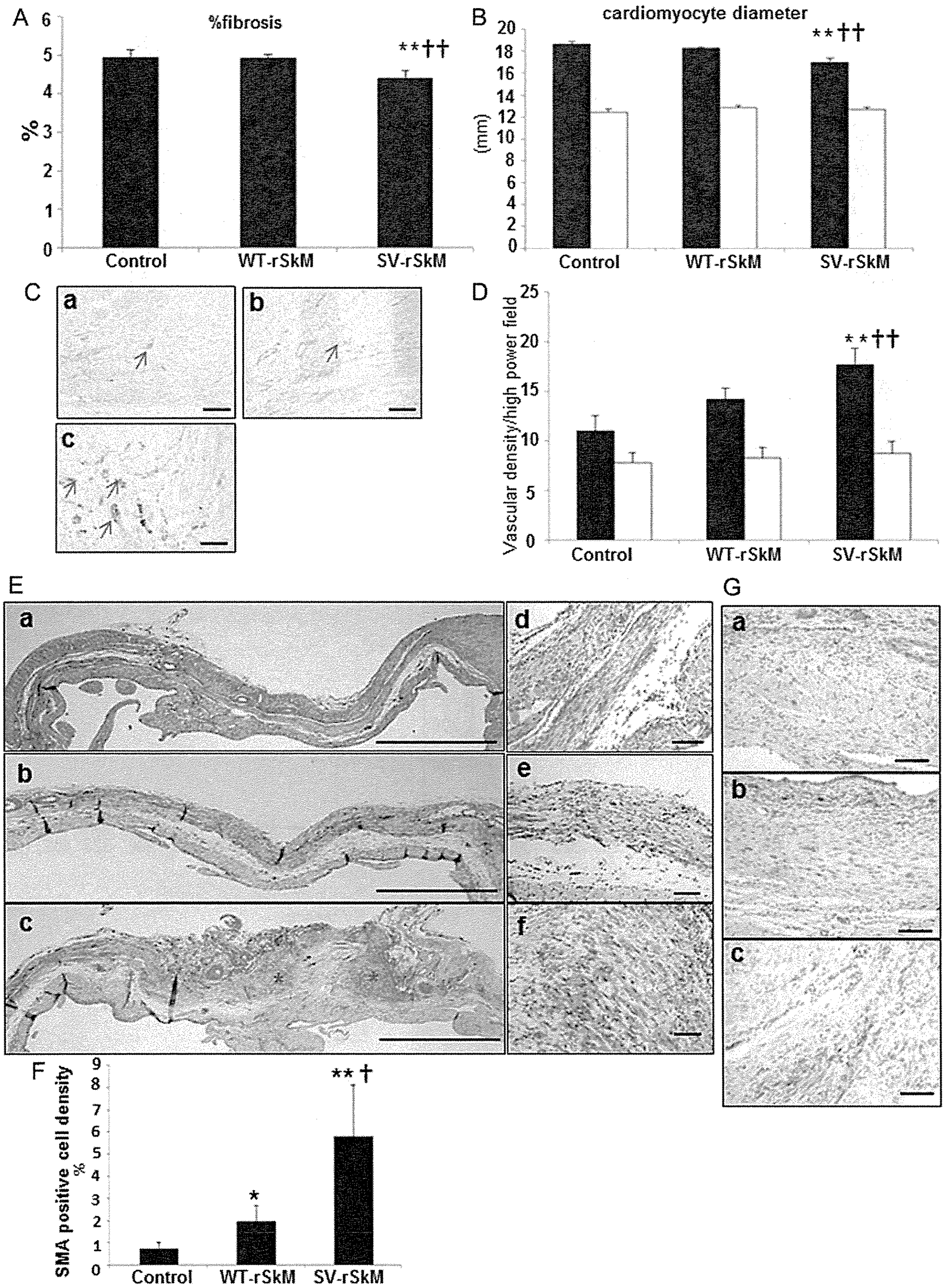

Figure 3 Histological evaluations of LV remodelling. (*A*) Percentage fibrosis. (*B*) Cardiomyocyte diameter. $^{**}P < 0.01$ vs. Control group. $^{\dagger\dagger}P < 0.01$ vs. WT-rSkM group. Filled bars, border area; open bars, remote area. Immunohistochemical staining. (*C*) A section of the infarcted border zone stained with an antibody against von Willebrand factor: (*a*) control; (*b*) WT-rSkM; and (*c*) SV-rSkM ($\times 200$ magnification, scale bars represent 100 μm). Newly formed vessel is stained brown. (*D*) Quantitative estimation of vascular density. $^{**}P < 0.01$ vs. Control group. $^{\dagger\dagger}P < 0.01$ vs. WT-rSkM group. Filled bars, border area; open bars, remote area. (*E*) The distribution of SMA-positive cells: (*a*) control; (*b*) WT-rSkM; (*c*) SV-rSkM (*a–c*, $\times 20$ magnification, scale bars represent 1000 μm; e and *f*, $\times 200$ magnification, scale bars represent 100 μm). Red asterisks denote SMA-positive cells. (*F*) Quantitative estimation of the SMA-positive cell density. $^{*}P < 0.05$, $^{**}P < 0.01$ vs. Control group. $^{\dagger}P < 0.05$ vs. WT-rSkM group. (*G*) The distribution of SM-MHC type 2-positive cells: (*a*) control; (*b*) WT-rSkM; and (*c*) SV-rSkM (*a–c*, $\times 200$ magnification, scale bars represent 100 μm).

Downloaded from http://cardiovascres.oxfordjournals.org/ at Osaka University on March 11, 2014

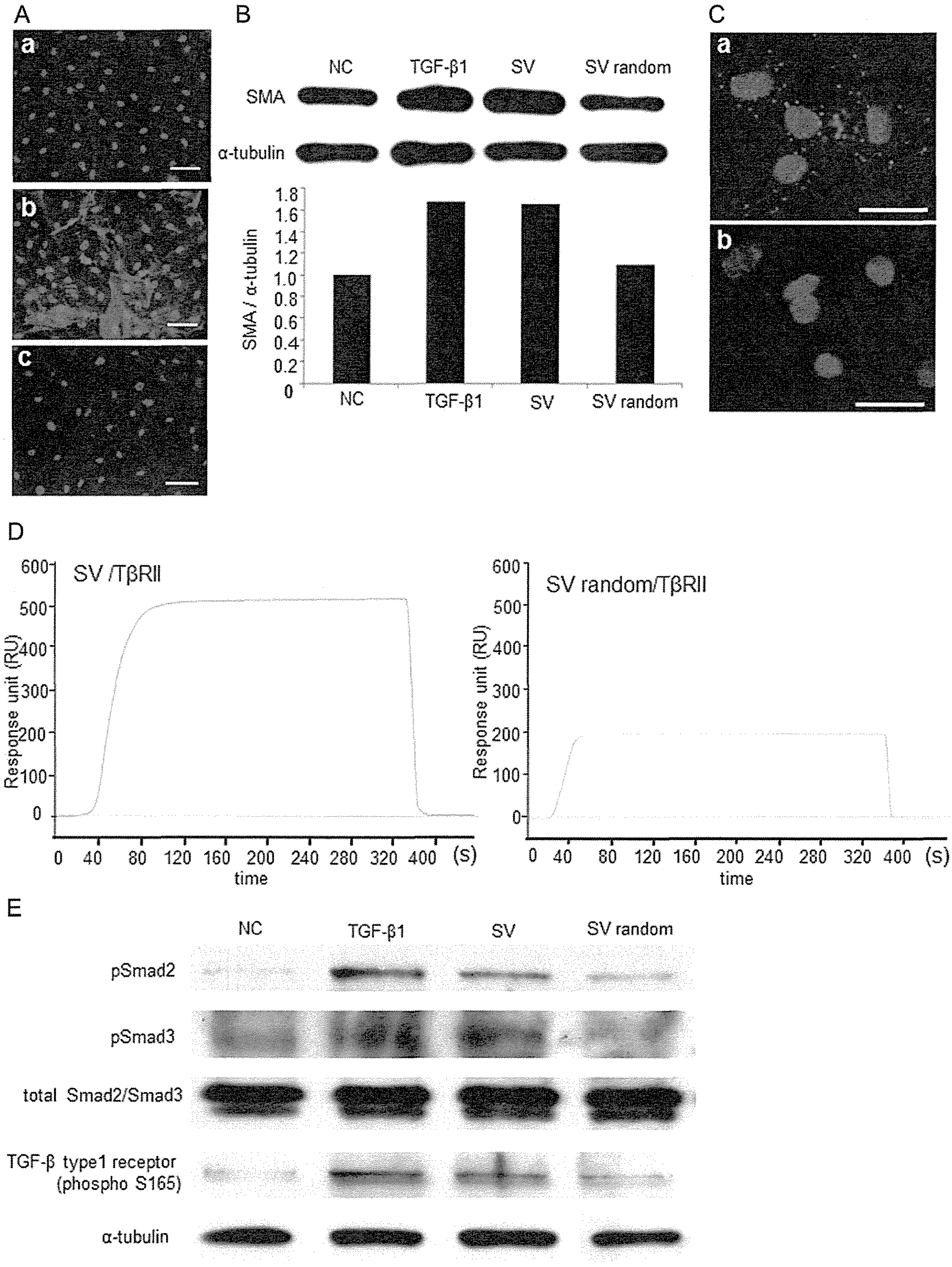

Figure 4 Myofibroblast differentiation induced by exposure of the isolated CFs to SV. (*A*) and (*B*) SMA expression induced by SV. (*A*) Immunofluorescence staining with an anti-SMA antibody: (*a*) non-stimulated CFs (NC); (*b*) CFs exposed to SV; and (*c*) CFs exposed to SV random peptide (×200 magnification, scale bars represent 100 μm). (*B*) Immunoblot of the myofibroblast differentiation marker SMA and its quantitative assessment. α-Tubulin was used as a loading control. (*C*) The examination of binding between TβRII and SV using an *in situ* PLA: (*a*) CFs exposed to SV; (*b*) CFs exposed to SV random peptide (scale bars represent 50 μm). The binding between TβRII and SV and the TGF-β–Smad signalling induced by SV. (*D*) Biacore analysis of the interaction of TβRII with SV. (*E*) Assessment of TGF-β–Smad signalling in CFs exposed to SV by western blotting. α-Tubulin was used as a loading control.

Downloaded from http://cardiovascres.oxfordjournals.org/ at Osaka University on March 11, 2014

3.8 Binding of SV to transforming growth factor-β receptor II

When PLA was performed using rabbit polyclonal anti-TβRII and mouse monoclonal anti-HA antibodies for the isolated fibroblasts treated with SV-HA peptide, PLA-positive red signals were found (*Figure 4C*[*a*]). In contrast, PLA-positive red signals were not detected in the isolated fibroblasts treated with SV-HA random peptide (*Figure 4C*[*b*]). We assessed the ability of SV to bind to TβRII, using a sensor chip immobilized with biotinylated SV ($K_D = 13.5$ nM), and this peptide bound to TβRII with high affinity (500 Resonance Unit; *Figure 4D*). However, SV random peptides ($K_D = 16$ nM) had a much lower R_{max} (R_{max} = analyte molecular weight (MW)/ligand MW × the immobilization level × the stoichiometric ratio) value (200 Resonance Unit).

3.9 The effects of SV on Smad activation

Treatment with TGF-β1 or SV induced the phosphorylation of TβRI, Smad2, and Smad3 to similar degrees (*Figure 4E*). Conversely, treatment with SV random peptide had no effect on TβRI, Smad2, and Smad3 phosphorylation.

4. Discussion

In this study, we transplanted myoblast sheets to the myocardium in an infarcted rat model. The cell sheets are removed from special temperature-responsive dishes without destroying the cell–cell or cell–extracellular matrix adhesions in the cell sheet. The myoblast sheet does not require an artificial scaffold, because it has a great ability to integrate with the infarcted area via an adhesion factor, such as integrin-$\alpha_7\beta_1$ and α-dystroglycan, which are expressed on the surface of myoblasts; thus, the sheets do not fall off after the chest is closed.[5–7]

The effect of myoblast sheet transplantation is mediated mainly by paracrine growth factors that stimulate the injured myocardium.[6,7] The paracrine effectors include HGF, VEGF, and stromal-derived factor 1. These factors can promote angiogenesis in the ischaemic myocardium. Hepatocyte growth factor is also associated with anti-fibrosis and anti-apoptosis. The grafted myoblasts beneficially attract haematopoietic stem cells to home in on the infarcted heart area for heart regeneration and angiogenesis by stromal-derived factor 1.[6] These paracrine activities induce angiogenesis and reduce fibrosis and hypertrophy; as a result, the depressed cardiac function improves. Therefore, we hypothesized that functional modification of myoblast sheet properties by overexpressing a factor associated with angiogenesis, anti-fibrosis, and anti-apoptosis could further promote and maintain the therapeutic effects of the sheet. Our previous results demonstrated that SV has a much stronger pro-angiogenic action than VEGF.[14] Given that SV has a straight-chain sequence, rather than a complicated conformation, we can speculate that this peptide would be degraded by peptidase within an organism. Our previous research has shown that synthetic SV has no effect on the proliferation of endothelial and muscle cells.[13,14] The degradation rate and function for the proliferation of SV could have high biocompatibility with peptides. In this study, we investigated the effects of SV-secreting myoblast sheets in infarcted rat hearts.

Most of the transplanted myoblasts drop out at 4 weeks after sheet transplantation.[21] As a result, cardiac function in the WT-rSkM group at 4 weeks after sheet transplantation was markedly decreased. In contrast, in the SV-rSkM group the functional improvements were maintained for 8 weeks after sheet transplantation. The capillary density 8 weeks after transplantation was significantly higher in the SV-rSkM group than in the control and WT-rSkM groups. The vessels newly formed by the secreted SVs from the myoblast sheets remained until 8 weeks post-transplantation, after the drop-out of the transplanted cells. The paracrine factors from transplanted myoblasts also promoted angiogenesis. Thus, in this study, the secreted SV showed an enhanced angiogenic action after myoblast transplantation. It is possible that SV induced angiogenesis in both the surviving cardiomyocytes and the transplanted cells; as a result, the survival time of the transplanted cells would have been extended. However, there are no data concerning the effect of SV-rSkM on the endogenous mobilization/proliferation/apoptosis and differentiation of cardiac resident cardiac stem/progenitor cells. More research is needed to define the effects of SV on these cells.

Siltanen *et al.*[11] reported the efficacy of a heart failure treatment involving the transplantation of myoblasts genetically modified to overexpress HGF. Hepatocyte growth factor is a cardioprotective factor associated with angiogenesis, anti-fibrosis, and anti-apoptosis.[22,23] Hepatocyte growth factor-overexpressing myoblast sheets stimulated angiogenesis and inhibited myocardial fibrosis in a rat chronic heart failure model. However, cardiac function was not improved by the transplantation of HGF-overexpressing sheets.[16] In contrast, SV-expressing sheets, which also have a pro-angiogenic action, enhanced cardiac function and angiogenesis. Transplantation of SV-secreting sheets enhanced the functional recovery of ischaemic myocardium compared with the findings in the control and WT-rSkM groups. In particular, systolic parameters, such as LVIDs and ESV, were significantly improved in the SV-rSkM group.

Myofibroblasts share morphological features with fibroblasts and smooth muscle cells. Differentiated myofibroblasts are characterized by increased α-SMA and the morphological features of well-developed stress fibres.[24] Although myofibroblasts in normal tissue, granulation tissue, and pathological tissue exhibit phenotypic α-SMA expression, SM-MHC, vimentin, and desmin, myofibroblasts more commonly express α-SMA.[25] Myofibroblasts have a greater contractile capability than undifferentiated CFs, and this property is believed to be important in maintaining the structural integrity of healing scars.[26] Expression of α-SMA in stress fibres is instrumental in force generation by myofibroblasts.[27] Additionally, myofibroblasts confer mechanical tension to remodelling matrix via anchoring and contracting.[24] In this study, many clusters of SMA-positive and SM-MHC type 2-positive cells were observed in infarcted areas in the SV-rSkM group. These cells differentiated from CFs into myofibroblasts in the infarcted area after the addition of SV, and the myocardial contractile performance of the infarcted wall in the SV-rSkM group was improved by the accumulation of myofibroblasts. Our previous study indicated that, when skeletal myoblast sheets were transplanted into a swine acute MI model, well-developed smooth muscle cells accumulated in the centre of the scar.[28] In our study, more SMA-positive cells accumulated in the infarcted area in the SV-rSkM group than in the WT-rSkM-group, and the secreted SV enhanced the effect of SMA expression by CFs. Furthermore, owing to the accumulation of myofibroblasts in the infarcted area, adverse effects on the uninjured myocardium and its exercise endurance were decreased; consequently, cardiac remodelling processes, such as fibrosis and cardiomyocyte hypertrophy, were attenuated. The fibroblasts in scar tissue of the infarcted area are differentiated into SMA-positive and SM-MHC type 2-positive cells by SV. There is no cell–cell connectivity between these cells and the recipient's cardiomyocytes, and it is possible that they have not been synchronized with the cardiomyocytes. However, they do have a contractile capability, and SV could have transferred the contractility to the infarcted wall via the

Downloaded from http://cardiovascres.oxfordjournals.org/ at Osaka University on March 11, 2014

accumulation of these cells, improving the motion of the scared left ventricular wall and inhibiting the dilatation of the LV chamber in the SV-rSkM group.

Our previous research has shown that synthetic SVVYGLR peptides *in vitro* activate the adhesion and migration of endothelial cells and smooth muscle cells, and stimulate tube formation by vascular endothelial cells.[13,14] In contrast, SV has no effect on the proliferation of these cells, whereas it enhances the adhesion and proliferation of several types of human mesenchymal cells.[17] Although the effects of SV on apoptosis in these cells have not been evaluated, the results regarding proliferation suggest that SV has no effect on apoptosis. According to these data, SV should have no impact on the proliferation and apoptosis of myoblasts, while stimulating the proliferation of fibroblasts and myofibroblasts.

Osteopontin is highly expressed during the differentiation of fibroblasts into myofibroblasts, and could have an effect on fibroblast differentiation and a role in myofibroblast function during tissue remodelling.[29] Transforming growth factor-β plays an important role in the activation of fibroblasts in wound repair, and it induces myofibroblast differentiation via Smad signalling.[30] Osteopontin is required for the differentiation and activation of myofibroblasts formed in response to TGF-β1.[31] This study illustrated that, in isolated CFs, SV had a great degree of affinity for TβRII and activated Smad signalling via TβRs. The secreted SV bound TβRII and induced the differentiation of fibroblasts into myofibroblasts through TGF-β receptor–Smad signalling.

Transforming growth factor-β participates in vascular development and the maintenance of vascular homeostasis, and it induces angiogenesis at low levels.[32] Transforming growth factor-β regulates angiogenesis by acting on both vascular endothelial and smooth muscle cells.[31] SV also stimulates angiogenesis at low levels, but this effect plateaus at high levels.[14] Thus, SV induces angiogenesis via the same mechanism as TGF-β. However, we believed that SV could also bind receptors other than TβRII and exhibit myocardium-protecting actions, such as promoting angiogenesis and inhibiting hypertrophy. To explain the effect of SV in improving cardiac function, SV receptors in myocardial tissue will have to be identified, and the details of its mechanism will need to be examined.

Functional SV peptide-secreting myoblast sheets facilitate long-term improvement in cardiac function and inhibition of cardiac remodelling. The SVs secreted from myoblast sheets effectively stimulated angiogenesis in the failing myocardium. The accumulation of SMA-positive cells induced by SV confers a contractile property on the infarcted wall. The early therapeutic effects after SV-secreting myoblast sheet transplantation were due to the paracrine effects of the transplanted myoblasts, and the late effects were caused by the pro-angiogenic effects of SV and its induction of myofibroblast accumulation via TGF-β–Smad signalling. These results suggest that SV could change CFs to muscle-like cells, allowing it to be used as a bridge to heart transplantation or as an ideal peptide drug for cardiac regeneration therapy.

Conflict of interest: none declared.

References

1. Buja LM, Vela D. Cardiomyocyte death and renewal in the normal and diseased heart. *Cardiovasc Pathol* 2008;**17**:349–374.
2. Gupta KB, Ratcliffe MB, Fallert MA, Edmunds LH Jr, Bogen DK. Changes in passive mechanical stiffness of myocardial tissue with aneurysm formation. *Circulation* 1994;**89**: 2315–2326.
3. Ciulla MM, Paliotti R, Ferrero S, Braidotti P, Esposito A, Gianelli U *et al.* Left ventricular remodeling after experimental myocardial cryoinjury in rats. *J Surg Res* 2004;**116**:91–97.
4. Okano T, Yamada N, Okuhara M, Sakai H, Sakurai Y. Mechanism of cell detachment from temperature-modulated, hydrophilic-hydrophobic polymer surfaces. *Biomaterials* 1995; **16**:297–303.
5. Kondoh H, Sawa Y, Miyagawa S, Sakakida-Kitagawa S, Memon IA, Kawaguchi N *et al.* Longer preservation of cardiac performance by sheet-shaped myoblast implantation in dilated cardiomyopathic hamsters. *Cardiovasc Res* 2006;**69**:466–475.
6. Memon IA, Sawa Y, Fukushima N, Matsumiya G, Miyagawa S, Taketani S *et al.* Repair of impaired myocardium by means of implantation of engineered autologous myoblast sheets. *J Thorac Cardiovasc Surg* 2005;**130**:1333–1341.
7. Miyagawa S, Sawa Y, Sakakida S, Taketani S, Kondoh H, Memon IA *et al.* Tissue cardiomyoplasty using bioengineered contractile cardiomyocyte sheets to repair damaged myocardium: their integration with recipient myocardium. *Transplantation* 2005;**80**: 1586–1595.
8. Memon IA, Sawa Y, Miyagawa S, Taketani S, Matsuda H. Combined autologous cellular cardiomyoplasty with skeletal myoblasts and bone marrow cells in canine hearts for ischemic cardiomyopathy. *J Thorac Cardiovasc Surg* 2005;**130**:646–653.
9. Narita T, Shintani Y, Ikebe C, Kaneko M, Harada N, Tshuma N *et al.* The use of cell-sheet technique eliminates arrhythmogenicity of skeletal myoblast-based therapy to the heart with enhanced therapeutic effects. *Int J Cardiol* 2012; pii: S0167-5273(12)01187-4. doi:10.1016/j.ijcard.2012.09.081. [Epub ahead of print].
10. Kitabayashi K, Siltanen A, Pätilä T, Mahar MA, Tikkanen I, Koponen J *et al.* Bcl-2 expression enhances myoblast sheet transplantation therapy for acute myocardial infarction. *Cell Transplant* 2010;**19**:573–588.
11. Siltanen A, Kitabayashi K, Lakkisto P, Mäkelä J, Pätilä T, Ono M *et al.* hHGF overexpression in myoblast sheets enhances their angiogenic potential in rat chronic heart failure. *PLoS One* 2011;**6**:e19161.
12. Sodek J, Ganss B, McKee MD. Osteopontin. *Crit Rev Oral Biol Med* 2000;**11**:279–303.
13. Hamada Y, Yuki K, Okazaki M, Fujitani W, Matsumoto T, Hashida MK *et al.* Osteopontin-derived peptide SVVYGLR induces angiogenesis *in vivo*. *Dent Mater J* 2004;**23**:650–655.
14. Hamada Y, Nokihara K, Okazaki M, Fujitani W, Matsumoto T, Matsuo M *et al.* Angiogenic activity of osteopontin-derived peptide SVVYGLR. *Biochem Biophys Res Commun* 2003; **310**:153–157.
15. Hamada Y, Egusa H, Kaneda Y, Hirata I, Kawaguchi N, Hirao T *et al.* Synthetic osteopontin-derived peptide SVVYGLR can induce neovascularization in artificial bone marrow scaffold biomaterials. *Dent Mater J* 2007;**26**:487–492.
16. Yokosaki Y, Matsuura N, Sasaki T, Murakami I, Schneider H, Higashiyama S *et al.* The integrin $\alpha_9\beta_1$ binds to a novel recognition sequence (SVVYGLR) in the thrombin-cleaved amino-terminal fragment of osteopontin. *J Biol Chem* 1999;**274**:36328–36334.
17. Egusa H, Kaneda Y, Akashi Y, Hamada Y, Matsumoto T, Saeki M *et al.* Enhanced bone regeneration via multimodal actions of synthetic peptide SVVYGLR on osteoprogenitors and osteoclasts. *Biomaterials* 2009;**30**:4676–4686.
18. Rissanen TT, Rutanen J, Ylä-Herttuala S. Gene transfer for therapeutic vascular growth in myocardial and peripheral ischemia. *Adv Genet* 2004;**52**:117–164.
19. Sack U, Hoffmann M, Zhao XJ, Chan KS, Hui DS, Gosse H *et al.* Vascular endothelial growth factor in pleural effusions of different origin. *Eur Respir J* 2005;**25**:600–604.
20. Kunig AM, Balasubramaniam V, Markham NE, Seedorf G, Gien J, Abman SH. Recombinant human VEGF treatment transiently increases lung edema but enhances lung structure after neonatal hyperoxia. *Am J Physiol Lung Cell Mol Physiol* 2006;**291**:L1068–L1078.
21. Saito S, Miyagawa S, Sakaguchi T, Imanishi Y, Iseoka H, Nishi H *et al.* Myoblast sheet can prevent the impairment of cardiac diastolic function and late remodeling after left ventricular restoration in ischemic cardiomyopathy. *Transplantation* 2012;**93**:1108–1115.
22. Nakamura Y, Morishita R, Higaki J, Kida I, Aoki M, Moriguchi A *et al.* Hepatocyte growth factor is a novel member of the endothelium-specific growth factors: additive stimulatory effect of hepatocyte growth factor with basic fibroblast growth factor but not with vascular endothelial growth factor. *J Hypertens* 1996;**14**:1067–1072.
23. Ono K, Matsumori A, Shioi T, Furukawa Y, Sasayama S. Enhanced expression of hepatocyte growth factor/c-Met by myocardial ischemia and reperfusion in a rat model. *Circulation* 1997;**95**:2552–2558.
24. Gabbiani G. The myofibroblast in wound healing and fibrocontractive diseases. *J Pathol* 2003;**200**:500–503.
25. Hinz B, Mastrangelo D, Iselin CE, Chaponnier C, Gabbiani G. Mechanical tension controls granulation tissue contractile activity and myofibroblast differentiation. *Am J Pathol* 2001;**159**:1009–1020.
26. Sun Y, Weber KT. RAS and connective tissue in the heart. *Int J Biochem Cell Biol* 2003;**35**: 919–931.
27. Hinz B, Celetta G, Tomasek JJ, Gabbiani G, Chaponnier C. Alpha-smooth muscle actin expression upregulates fibroblast contractile activity. *Mol Biol Cell* 2001;**12**:2730–2741.
28. Miyagawa S, Saito A, Sakaguchi T, Yoshikawa Y, Yamauchi T, Imanishi Y *et al.* Impaired myocardium regeneration with skeletal cell sheets—a preclinical trial for tissue-engineered regeneration therapy. *Transplantation* 2010;**90**:364–372.
29. Pereira RO, Carvalho SN, Stumbo AC, Rodrigues CA, Porto LC, Moura AS *et al.* Osteopontin expression in coculture of differentiating rat fetal skeletal fibroblasts and myoblasts. *In Vitro Cell Dev Biol Anim* 2006;**42**:4–7.
30. Dobaczewski M, Bujak M, Li N, Gonzalez-Quesada C, Mendoza LH, Wang XF *et al.* Smad3 signaling critically regulates fibroblast phenotype and function in healing myocardial infarction. *Circ Res* 2010;**107**:418–428.
31. Lenga Y, Koh A, Perera AS, McCulloch CA, Sodek J, Zohar R. Osteopontin expression is required for myofibroblast differentiation. *Circ Res* 2008;**102**:319–327.
32. Orlova VV, Liu Z, Goumans MJ, ten Dijke P. Controlling angiogenesis by two unique TGF-β type I receptor signaling pathways. *Histol Histopathol* 2011;**26**:1219–1230.

Downloaded from http://cardiovascres.oxfordjournals.org/ at Osaka University on March 11, 2014

Copyright © 2013 Cognizant Communication Corporation

DOI: 10.3727/096368913X665602

CT-0968 Accepted 03/17/2013 for publication in "*Cell Transplantation*"

Improvement of Cardiac Stem Cell-Sheet Therapy for Chronic Ischemic Injury by Adding Endothelial Progenitor Cell Transplantation: Analysis of Layer-Specific Regional Cardiac Function

Sokichi Kamata[1], Shigeru Miyagawa[1], Satsuki Fukushima[1], Satoshi Nakatani[2], Atsuhiko Kawamoto[3], Atsuhiro Saito[1], Akima Harada[1], Tatsuya Shimizu[4], Takashi Daimon[5], Teruo Okano[4], Takayuki Asahara[3], Yoshiki Sawa[1,*]

[1]Department of Cardiovascular Surgery, Osaka University Graduate School of Medicine, Suita, Japan

[2] Division of Functional Diagnostics, Department of Cardiovascular Medicine, Osaka University Graduate School of Medicine, Suita, Japan

[3] Division of Vascular Regeneration Therapy, Institute of Biomedical Research and Innovation, Kobe, Japan

[4] Institute of Advanced Biomedical Engineering and Science, Tokyo Women's Medical University, Tokyo, Japan

[5]Department of Biostatistics, Hyogo College of Medicine, Nishinomiya, Hyogo, Japan

Running title: Combined CSC sheet and EPC Therapy for ICM

Address for Correspondence:
Professor Yoshiki Sawa,
Department of Cardiovascular Surgery, Osaka University Graduate School of Medicine,
2-2 Yamadaoka, Suita, Osaka, 565-0871, Japan
Tel: +81 6 6879 3154, **Fax:** +81 6 6879 3163
E-mail: sawa-p@surg1.med.osaka-u.ac.jp

Word count: Abstract: 300 ;body text: 7,903

Copyright © 2013 Cognizant Communication Corporation

ABSTRACT

BACKGROUND: The transplantation of cardiac stem cell sheets (CSC sheets) is a promising therapeutic strategy for ischemic cardiomyopathy, although potential ischemia in the transplanted area remains a problem. Injected endothelial progenitor cells (EPCs) can reportedly induce angiogenesis in the injected area. We hypothesized that concomitant CSC sheet transplantation and EPC injection might show better therapeutic effects for chronic ischemic injury model than the transplantation of CSC sheets alone.

METHODS: Scaffold-free CSC-sheets were generated from human c-kit-positive heart-derived cells. A porcine chronic ischemic injury model was generated by placing an ameroid constrictor around the left coronary artery for 4 weeks. The animals then underwent a sham operation, epicardial transplantation of CSC sheet over the ischemic area, intramyocardial injection of EPCs into the ischemic and peri-ischemic area, or CSC-sheet transplantation plus EPC injection. The efficacy of each treatment was then assessed for 2 months.

RESULTS: Speckle-tracking echocardiography was used to dissect the layer-specific regional systolic function by measuring the radial strain (RS). The epicardial RS in the ischemic area was similarly greater after treatment with the CSC-derived cell-sheets alone (19±5%) or in combination with EPC injection (20±5%) compared with the EPC only (9±4%) or sham (7±1%) treatment. The endocardial RS in the ischemic area was greatest after the combined treatment (14±1%), followed by EPC only (12±1%), compared to the CSC only (11±1%) and sham (9±1%) treatments. Consistently, either epicardial CSC-sheet implantation or intramyocardial EPC injection yielded increased capillary number and reduced cardiac fibrosis in the ischemic epicardium or endocardium, respectively. Concomitant EPC injection induced the migration of transplanted CSCs into the host

Copyright © 2013 Cognizant Communication Corporation

myocardium, leading to further neovascularization and reduced fibrosis in the ischemic endocardium, compared to the CSC-sole therapy.

CONCLUSION: Transplantation of CSC-sheets induced significant functional recovery of the ischemic epicardium, and concomitant EPC transplantation elicited transmural improvement in chronic ischemic injury.

Key-words: Cardiac stem cell, Endothelial progenitor cell, Chronic ischemic injury, Strain imaging, Left ventricular remodeling

BACKGROUND

Transplantation of somatic tissue-derived stem cells has been shown to be a feasible, safe, and potentially effective treatment for advanced cardiac failure in clinical settings (6,32). In particular, cardiac stem cells (CSCs), represented by c-kit-positive cells in the myocardium, can play a central role in healing the damaged myocardium, through their direct differentiation *in situ*, the recruitment of circulating stem/progenitor cells, or the paracrine release of cardioprotective factors (9,12,30). CSC transplantation is therefore considered a promising treatment for advanced cardiac failure, although the optimal method for cell delivery into the heart is still under debate (7).

The transplantation of scaffold-free cell sheets was shown to enhance the retention and survival of the transplanted cells and to minimize the risks of cell-delivery-related myocardial damage that leads to arrhythmogenicity, thus showing good therapeutic potential (5,20,33). However, concerns remain regarding the integration of the transplanted cells into the myocardium, which would have a direct impact on regional cardiac function, and the

Copyright © 2013 Cognizant Communication Corporation

potential for ischemia in the transplanted cell sheet, which would limit its therapeutic potential. On the other hand, endothelial progenitor cells (EPCs) have been shown to induce neo-angiogenesis in the ischemic/infarcted myocardium and to activate residential CSCs to enhance healing and/or regeneration of the damaged myocardium (11,13,31). The intramyocardial injection of EPCs is thus another promising treatment for enhancing myocardial regeneration and possibly supporting the cellular function of transplanted CSCs (16).

We thus hypothesized that CSC transplantation by the cell-sheet technique might induce cardiomyogenic differentiation *in situ*, reverse left ventricular (LV) remodeling, and improve functional recovery in ischemic injury model and that these therapeutic effects might be enhanced by the concomitant transplantation of EPCs, which could have different effects on the damaged myocardium from CSCs.

Several lines of evidence suggested that region-specific, especially layer-specific, LV function assessed by recently-developing modalities may be superior to globally-measured ejection fraction (EF) in predicting myocardial recovery after a wide range of medical and surgical treatment (3,14). Here we used a porcine chronic ischemic injury model to dissect the layer-specific functional effects of these two types of cell transplantation.

Copyright © 2013 Cognizant Communication Corporation

METHODS

All human and animal studies were carried out with the approval of the institutional ethical committee. Human samples were collected under written informed consent. The investigation conforms to the Principles of Laboratory Animal Care formulated by the National Society for Medical Research and the Guide for the Care and Use of Laboratory Animals (US National Institutes of Health Publication No. 85-23, revised 1996). All experimental procedures and evaluations were carried out in a blinded manner.

Isolation and cultivation of c-kit-positive cells from human cardiac tissue

Human normal right atrial tissues were obtained from a 53-year-old female patient with dilated cardiomyopathy at Osaka University Hospital. The isolation method was as published recently (6). Briefly, after dissecting fat and fibrous tissue, the sample were cut into small pieces (< 1 mm^3) and suspended in 8 ml Ham's F12 medium (Wako Pure Chemical Inc., Osaka, Japan) containing 0.2% collagenase (17454, Serva Electrophoresis, Heidelberg, Germany). After digestion, cells were plated in culture dishes (353003, BD Falcon, Franklin Lakes, NJ) containing Ham's F12 supplemented with 10% FBS (SH30406.02, Hyclone, Thermo Scientific, Waltham, MA), 10ng/ml recombinant human basic fibrobrast growth factor (bFGF) (100-18B, PeproTech, Rocky Hill, NJ), 0.2 mM L-Glutathione (G6013, Sigma Aldrich, St Louis, MO) and 5 mU/ml erythropoietin (E5627-10UN, Sigma Aldrich). Subsequently, cells were expanded and subjected to fluorescence activated cell sorting (FACSAria) with antibody (CD117(AC126)-PE, 130-091-735, Miltenyi Biotec, Bergisch Gladbach, Germany) to obtain C-Kit positive CSCs. The sorted c-kit-positive CSCs were cultured until the fifth passage in medium containing Ham's F-12, 10% fetal bovine serum

Copyright © 2013 Cognizant Communication Corporation

(SH30406.02, Hyclone, Thermo Fisher Scientific), 0.2 mM L-Glutathione (G6013, Sigma Aldrich), 10 ng/ml recombinant human bFGF (100-18B, PeproTech), and 5 mU/ml erythropoietin (E5627-10UN, Sigma Aldrich) (30).

Preparation of CSC sheet and endothelial progenitor cells

Cultured CSCs were characterized by fluorescence-activated cell sorting (FACS) analysis, labeled by DiI-red (Molecular Probes, Eugene, OR) (33), and then incubated on 10-cm thermoresponsive dishes (Cell Seed Inc., Tokyo, Japan) at 37°C for 12 hours. The DiI-red labeled CSCs spontaneously detached from the dish surface following incubation at 20°C for 30 minutes, yielding a CSC sheet. Each CSC sheet was approximately 42 mm in diameter and 100-μm thick. Granulocyte colony stimulating factor-mobilized EPCs of human origin (AllCells, MPB-017F, Emeryville, CA) were labeled with DiI-blue *in vitro* (Molecular Probes) (33). The following monoclonal antibodies were used: C-kit APC (A3C6E2(clone), 130-091-733, Miltenyi Biotec), CD105 PE (FAB10971P, R&D Systems, Minneapolis, MN), CD34 FITC (555821, BD Biosicences), CD31 PE (FAB3567P, R&D Systems), 7AAD PerCP-Cy5-5 (51-68981E(559925), BD Biosicences), IgG1-FITC isotype controls (555748, BD Biosicences), IgG1-APC isotype controls (130-092-214, Miltenyi Biotec), and IgG1-PE isotype controls (IC002P, R&D Systems).

Generation of the swine chronic ischemic injury model and cell transplantation

A 2.5-mm ameroid constrictor (Tokyo Instruments, Inc, Tokyo, Japan) was placed around the proximal left anterior descending artery *via* a left thoracotomy in female swine (Clawn miniature, 1-year-old, 25kg) (Japan Farm, Inc, Kagoshima, Japan). A total of 65 swines were

Copyright © 2013 Cognizant Communication Corporation

then cared for in a temperature-controlled individual cage with a daily intake of 5 mg/kg cyclosporin A (Novartis, East Hanover, NJ) (15). Multi-detector CT identified 52 pigs that developed an LVEF between 30 and 40% at 21 days post-ameroid placement. Since eight of these pigs died prior to cell transplantation, so a total of 44 pigs were randomly divided into 4 treatment groups (n=11 in each): sham operation (sham group), CSC-sheet transplantation only (CSC-only group), intramyocardial injection of EPCs (EPC-only group), and CSC-sheet transplantation plus EPC injection (CSC-EPC group). After a median sternotomy under general anesthesia, 3-layered CSC sheet (total 1×10^8 cells) was placed on the epicardium of the ischemic area (LAD region), and stitched in place around the edge. EPCs (total 2.5×10^6 cells) were intramyocardially injected into 12 different sites of the ischemic and peri-ischemic area. After the transplantation and/or intramyocardial injection was completed, the pericardium was closed. The pigs were taken care of for 1 day (n=1 each), 3 (n=4 each) or 8 weeks (n=6 each), when they were sacrificed in a humane manner.

CELL TRANSPLANTATION The Regenerative Medicine Journal

Continuous electrocardiogram monitoring

The electrocardiogram (ECG) was monitored during 5 days post-treatment with the Holter system (Unique Medical Co, Tokyo, Japan) for swines sacrificed at 8 weeks after cell transplantation (n=6 each group). The heart rate and arrhythmia events during the first 24 hours were analyzed using software (Softron Co, Tokyo, Japan).

Multi-detector CT and conductance catheterization

Global LV function was assessed by multi-detector CT at pre-treatment and 8 weeks post-treatment (n=6 each), and by cardiac catheterization at 8 weeks post-treatment (n=5 each).

Copyright © 2013 Cognizant Communication Corporation

After infusing 45 mL of nonionic contrast agent (Iomeron 350, Eisai, Co, Tokyo, Japan) *via* the ear vein, 5-mm slice images of the entire heart were obtained in the cranio-caudal direction using a 16-slice CT scanner (Emotion 16, Siemens, Tokyo, Japan). Every 10% of the R-R interval was reconstructed to calculate the LVEF and end-diastolic/systolic volume (EDV and ESV, respectively) using software (Lexus, Aze Inc, Tokyo, Japan).

Pressure-volume (P-V) cardiac catheterization was performed after median sternotomy by inserting a conductance catheter (Unique Medical) and a Micro Tip catheter transducer (SPR-671; Millar Instruments, Inc, Houston, Tex) into the LV cavity. The P-V loop data under stable hemodynamics or inferior vena cava occlusion were analyzed with Integral 3 software (Unique Medical).

Speckle-tracking echocardiography and myocardial contrast echocardiography

Short-axis echocardiographic images, obtained using the Artida 4D Echocardiography System (Toshiba Medical Systems Co, Tochigi, Japan) and PST-30SBT transducer, were analyzed by the speckle-tracking method using wall motion tracking software (Toshiba Medical Systems) (2,4). End-systolic radial strain (RS) values at the mid and apical levels were averaged in a layer-specific manner to measure the endocardial and epicardial wall motion index (WMI), respectively.

Myocardial contrast echocardiography was performed using real-time contrast pulse sequencing operating on the Aplio ultrasound system (Toshiba Medical Systems) (8). Briefly, after an intravenous injection of 20 mL of ultrasound contrast agent (Sonazoid, Daiichi Sankyo Inc, Parsippany, NJ), images in the apical 2-chamber view were acquired to score the myocardial opacification using Volmac software (YD Ltd, Nara, Japan).

Copyright © 2013 Cognizant Communication Corporation

Histology

Cultured CSCs on 8-well Lab-Tec chamber slides were fixed with 4% paraformaldehyde, labeled, and examined by confocal microscopy (FV300, Olympus, Tokyo, Japan). AlexaFluor-488 Phalloidin (Molecular Probes) was used to enhance the background actin filaments. Paraffin-embedded transverse sections at the papillary muscle level was stained with Masson's trichrome, and the amount of interstitial collagen at the entire LV wall was semi-quantified by MetaMorph software (Molecular Devices, Sunnyvale, CA) (n=6, in each). In addition, the thickness of the ventricular wall was measured at two points from the LV posterior area and two points from the interventricular septum, and results were expressed as the average of the four points. Five-micrometer cryo-sections were subjected to either periodic acid-Schiff (PAS) staining or immunohistolabeling. The following primary antibodies were used: rabbit anti-c-kit (Dako, Co, Glostrup, Denmark), mouse anti-smooth muscle actin (Dako), rabbit anti-von Willebrand factor (vWF) (Dako), mouse anti-ki67 (Dako), rabbit anti-connexin 43 (Sigma Aldrich), mouse anti-cardiac troponin I (cTn-I) (Abcam, Co, Cambridge, UK), mouse anti-stromal cell-derived factor 1 (SDF-1) (Abcam), rabbit anti-vascular endothelial growth factor (VEGF) (Thermo Scientific), rabbit anti-insulin-like growth factor 1 (IGF-1) (Abcam). Capillary density was expressed as the average number of vWF-positive circular structures in five randomly selected sections, corrected for the total area of the tissue section measured. PAS-stained sections were used to determine the cell diameter of the cardiomyocytes at the remote zone. Dil-red positive cells were traced by MetaMorph software to quantify the area of engrafted clusters of CSC sheet.